

Ticagrelor alters the membrane of *Staphylococcus aureus* and enhances the activity of vancomycin and daptomycin without eliciting cross-resistance

Kirsten Leeten,¹ Nicolas Jacques,¹ Lidia Alejo Esquembre,² Dana C. Schneider,² Jan Straetener,² Camilla Henriksen,³ Lucia Musumeci,¹ Florence Putters,¹ Sofia Melo,¹ Elena Sánchez-López,⁴ Martin Giera,⁴ Noémie Penoy,⁵ Géraldine Piel,⁵ Olivier Verlaine,⁶ Ana Amoroso,⁶ Bernard Joris,⁶ Christoph J. Slavetinsky,^{7,8,9} Eric Goffin,¹⁰ Bernard Pirotte,¹⁰ Dorte Frees,³ Heike Brötz-Oesterhelt,^{2,8,9} Patrizio Lancellotti,¹ Cécile Oury¹

AUTHOR AFFILIATIONS See affiliation list on p. 17.

ABSTRACT Infections with multidrug-resistant bacteria pose a major healthcare problem which urges the need for novel treatment options. Besides its potent antiplatelet properties, ticagrelor has antibacterial activity against Gram-positive bacteria, including methicillin- and vancomycin-resistant *Staphylococcus aureus* (MRSA and VRSA). Several retrospective studies in cardiovascular patients support an antibacterial effect of this drug which is not related to its antiplatelet activity. We investigated the mechanism of action of ticagrelor in *Staphylococcus aureus* and model *Bacillus subtilis*, and assessed cross-resistance with two conventional anti-MRSA antibiotics, vancomycin and daptomycin. *Bacillus subtilis* bioreporter strains revealed ticagrelor-induced cell envelope-related stress responses. Sub-inhibitory drug concentrations caused membrane depolarization, impaired positioning of both the peripheral membrane protein MinD and the peptidoglycan precursor lipid II, and it affected cell shape. At the MIC, ticagrelor destroyed membrane integrity, indicated by the influx of membrane impermeable dyes, and lipid aggregate formation. Whole-genome sequencing of *in vitro*-generated ticagrelor-resistant MRSA clones revealed mutations in genes encoding ClpP, ClpX, and YjbH. Lipidomic analysis of resistant clones displayed changes in levels of the most abundant lipids of the *Staphylococcus aureus* membrane, for example, cardiolipins, phosphatidylglycerols, and diacylglycerols. Exogenous cardiolipin, phosphatidylglycerol, or diacylglycerol antagonized the antibacterial properties of ticagrelor. Ticagrelor enhanced MRSA growth inhibition and killing by vancomycin and daptomycin in both exponential and stationary phases. Finally, no cross-resistance was observed between ticagrelor and daptomycin, or vancomycin. Our study demonstrates that ticagrelor targets multiple lipids in the cytoplasmic membrane of Gram-positive bacteria, thereby retaining activity against multidrug-resistant *staphylococci* including daptomycin- and vancomycin-resistant strains.

IMPORTANCE Infections with multidrug-resistant bacteria pose a major healthcare problem with an urgent need for novel treatment options. The antiplatelet drug ticagrelor possesses antibacterial activity against Gram-positive bacteria including methicillin-resistant and vancomycin-resistant *Staphylococcus aureus* strains. We report a unique, dose-dependent, antibacterial mechanism of action of ticagrelor, which alters the properties and integrity of the bacterial cytoplasmic membrane. Ticagrelor retains activity against multidrug-resistant staphylococci, including isolates carrying the most common *in vivo* selected daptomycin resistance mutations and vancomycin-intermediate *Staphylococcus aureus*. Our data support the use of ticagrelor as adjunct therapy against multidrug-resistant strains. Because of the presence of multiple non-protein

Editor Marthie M. Ehlers, University of Pretoria, Pretoria, Gauteng, South Africa

Address correspondence to Cécile Oury, cecile.oury@uliege.be, or Heike Brötz-Oesterhelt, heike.broetz-oesterhelt@uni-tuebingen.de.

The authors declare no conflict of interest.

See the funding table on p. 17.

Received 30 April 2024

Accepted 19 August 2024

Published 23 September 2024

Copyright © 2024 Leeten et al. This is an open-access article distributed under the terms of the [Creative Commons Attribution 4.0 International license](https://creativecommons.org/licenses/by/4.0/).

targets of this drug within the bacterial membrane, resistance development is expected to be slow. All these findings corroborate the accumulating observational clinical evidence for a beneficial anti-bacterial effect of ticagrelor in cardiovascular patients in need of such treatment.

KEYWORDS Gram-positive bacteria, drug discovery, drug interactions, platelets

Infections with multidrug-resistant (MDR) bacteria are a major healthcare problem with prolonged hospitalization and increased mortality (1). In 2019, around 4.95 million deaths worldwide were reported to be related to antimicrobial resistance of which more than 100,000 were attributed to methicillin-resistant *Staphylococcus aureus* (MRSA) (2). The increasing infection rate with MDR bacteria urges the need for novel treatment options to overcome the problem of untreatable MDR bacterial infections. An emerging avenue of interest involves the repurposing of existing drugs for tackling MDR infections.

One such potential drug that has recently garnered interest is the cyclopentyl-triazolopyrimidine antiplatelet drug ticagrelor. The reversible P2Y₁₂ inhibitor is currently used to prevent cardiovascular events in patients with coronary artery disease (3, 4). Besides its potent antiplatelet properties, a sub-analysis of the PLATO trial comparing ticagrelor and clopidogrel in acute coronary syndrome patients revealed a lower risk of infection-related death upon treatment with ticagrelor (5). This was further supported by the XANTHIPPE study, showing that pneumonia patients experienced enhanced lung function after receiving ticagrelor treatment (6). Following these clinical observations, our team found that ticagrelor has antibacterial activity *in vitro* against Gram-positive and resistant Gram-positive bacteria such as MRSA and methicillin-resistant *Staphylococcus epidermidis* (MRSE) with minimal inhibitory concentrations (MIC) of 20 µg/mL (7, 8). Although 20 µg/mL ticagrelor is above the plasma concentrations reached in conventionally dosed patients, several beneficial effects have been reported at conventional doses that could explain the *in vivo* observations in patients. Our team has shown that ticagrelor at a conventional dose (1 µg/mL) alters *S. aureus* virulence and downregulates essential factors of the accessory gene regulator (*agr*) system, without affecting bacterial growth. Accordingly, at this dosage, ticagrelor was able to prevent infective endocarditis development in mice while clopidogrel had no effect (9). Moreover, treatment with ticagrelor cured an *S. aureus* infection in a mouse model of prosthetic joint infection, with downregulation of biofilm-related genes (10). These results were further supported by several retrospective clinical studies showing a 1-year lower risk of *S. aureus* bacteremia in acute coronary syndrome patients on ticagrelor compared to clopidogrel (11, 12).

Despite compelling evidence for the antibacterial activity of ticagrelor in addition to its role as a potent antiplatelet drug, its mechanism of action against Gram-positive bacteria remains to be elucidated. The present study aims to identify ticagrelor targets in MRSA and *B. subtilis* and assess its interaction with conventionally used mainstays of anti-staphylococcal therapy, daptomycin and vancomycin. The activity of ticagrelor against daptomycin and vancomycin-resistant strains was also investigated.

RESULTS

Ticagrelor induces cell envelope stress responses

To narrow down on the cellular structure or metabolic pathway primarily affected by ticagrelor in Gram-positive bacteria, we used a set of five luciferase bioreporter strains in the model species *B. subtilis* which were previously validated with an antibiotic reference library (13). Reporter strains were treated with ticagrelor (0.08 µg/mL to 80 µg/mL) in liquid culture in microtiter plates parallel to reference antibiotics, which were applied in their respective inducing concentration ranges. The cell envelope stress biomarker *ypuA* was induced by 2.5 and 5 µg/mL ticagrelor and a wide range of ticagrelor concentrations (1.25–80 µg/mL) induced the lipid II cycle stress biomarker *lial* (Fig. 1). In agreement with previous studies (13, 14), these two biomarkers were also triggered by both daptomycin and vancomycin. No induction was observed for the biomarkers of

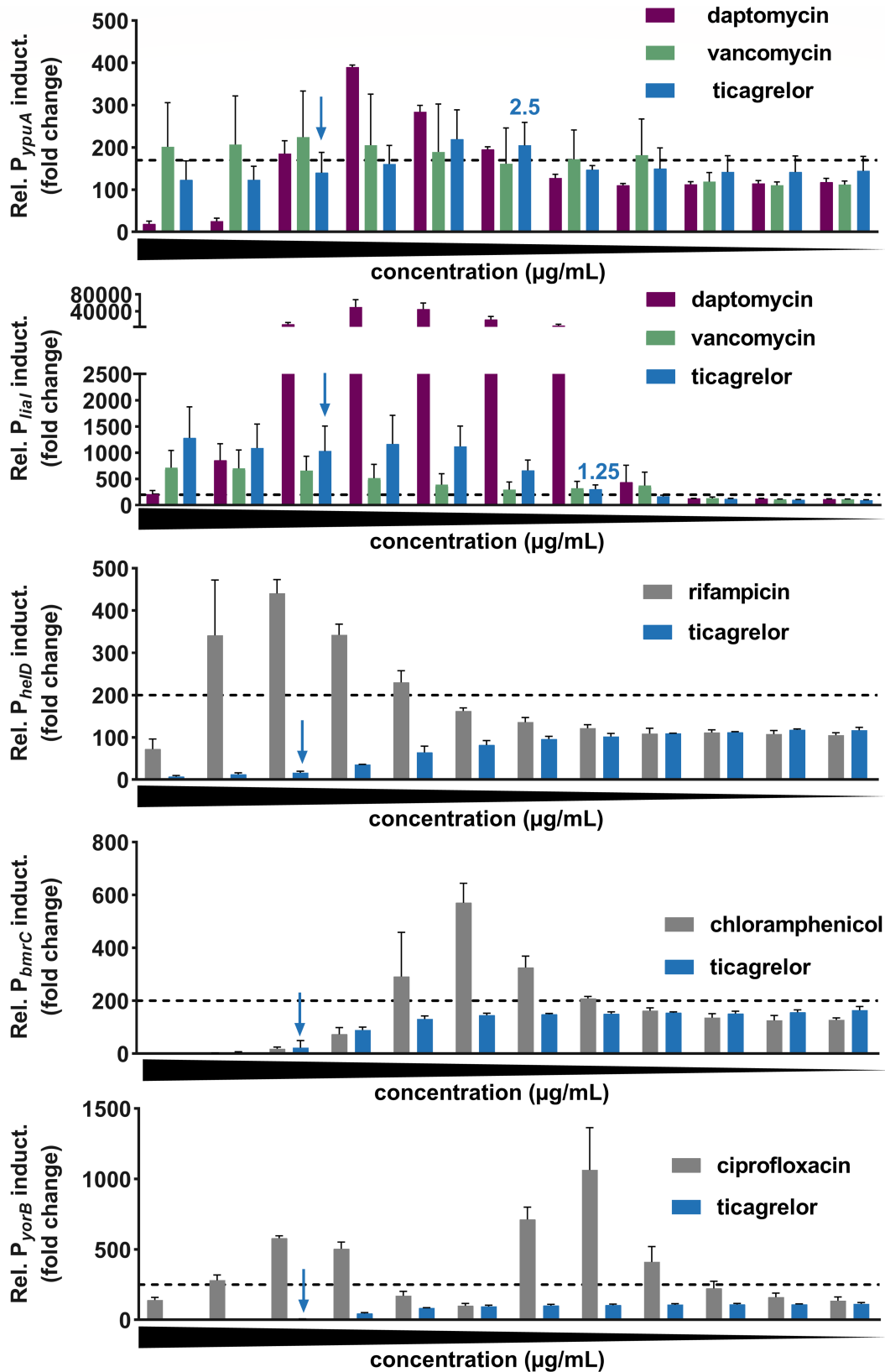


FIG 1 Ticagrelor induces cell envelope-related stress responses in *Bacillus subtilis*. Luciferase-based bioreporter assay using the sporulation-deficient *B. subtilis* 1534 *luc* reporter strains for *ypuA*, *lial*, *helD*, *bmrC*, and *yorB*. Luminescence signals are depicted in % of a control culture, that is, 100% corresponding to the background luminescence level in untreated cells. In a previous study using a large set of reference antibiotics with established modes of action, the threshold (Continued on next page)

Fig 1 (Continued)

values for a significant mode of action-based promotor induction were validated and set to the following promotor-specific threshold values which are indicated by dashed lines (13): 170% for *ypuA* (cell envelope stress) ($N = 6$), 250% for *yorB* (DNA stress) ($N = 2$), and 200% for *lial* (lipid-II cycle stress) ($N = 7$), *helD* (RNA stress) ($N = 3$), and *bmrC* (translational arrest) ($N = 2$). Twofold serial dilutions of compounds from left to right. Ticagrelor from 80 $\mu\text{g}/\text{mL}$ to 0.08 $\mu\text{g}/\text{mL}$, daptomycin from 32 $\mu\text{g}/\text{mL}$ to 0.04 $\mu\text{g}/\text{mL}$, vancomycin from 16 $\mu\text{g}/\text{mL}$ to 0.02 $\mu\text{g}/\text{mL}$, rifampicin from 0.006 $\mu\text{g}/\text{mL}$ to 0.000003 $\mu\text{g}/\text{mL}$, chloramphenicol from 25 $\mu\text{g}/\text{mL}$ to 0.01 $\mu\text{g}/\text{mL}$, and ciprofloxacin from 6.25 $\mu\text{g}/\text{mL}$ to 0.003 $\mu\text{g}/\text{mL}$. Graphs represent mean \pm SD. The lowest ticagrelor concentration causing induction above the threshold is indicated in blue. Blue arrows mark the MIC concentration of ticagrelor (20 $\mu\text{g}/\text{mL}$).

RNA stress (*helD*), translation arrest (*bmrC*), or DNA stress, that is, strand breaks (*yorB*) in contrast to rifampicin, chloramphenicol, and ciprofloxacin, respectively. These results were corroborated in an independent assay format (14) with *B. subtilis* lacZ bioreporter strains (Fig. S1). These data showed that ticagrelor induces cell envelope stress responses, at concentrations below the MIC (20 $\mu\text{g}/\text{mL}$) (Fig. S2A).

Ticagrelor alters membrane properties of *B. subtilis* and MRSA

We then assessed whether ticagrelor alters the structure or function of the bacterial cytoplasmic membrane using *B. subtilis* and the MRSA strain USA300 JE2. We followed the membrane potential over 15 min using the potential-sensitive fluorescent dye diethyloxycarbocyanine iodide [DiOC₂(3)]. Ticagrelor triggered a dose dependent and immediate drop of membrane potential in *B. subtilis* (Fig. 2A). Similarly, the membrane potential in MRSA JE2 (Fig. 2B) and MSSA (data not shown) was affected within minutes. For both strains, ticagrelor-induced membrane depolarization reached levels comparable to those obtained with the positive control protonophore, carbonyl cyanide *m*-chlorophenyl hydrazone (CCCP). Notably, membrane depolarization was induced by sub-inhibitory concentrations of ticagrelor. While the same MIC of 20 $\mu\text{g}/\text{mL}$ was obtained for *B. subtilis* and several *S. aureus* strains (MRSA and MSSA) (Fig. S2A through D), effects on the membrane potential were already significant at 2.5 $\mu\text{g}/\text{mL}$ for *B. subtilis* and at 10 $\mu\text{g}/\text{mL}$ for MRSA USA300 JE2 (Fig. 2A and B). These data were supported by microscopic analyses in a *B. subtilis* strain expressing a GFP-tagged MinD protein (15). This peripheral membrane protein indeed delocalizes upon membrane potential dissipation (15). Delocalization of MinD occurred at 10 $\mu\text{g}/\text{mL}$ ticagrelor, and further increased at the MIC (Fig. 2C). As MinD is important for properly positioning the cell division machinery in *B. subtilis* (15), its displacement results in disturbed divisome placement (15). Probing for further topological disturbances, we monitored the position of BODIPY FL-vancomycin, which targets the D-ala D-ala moieties in the peptidoglycan layer and the membrane-bound peptidoglycan precursor lipid II (16). Due to increased peptidoglycan *de novo* synthesis, the septal region contains elevated lipid II levels (17) and is brightly and regularly labeled by BODIPY FL-vancomycin in control cells (Fig. S3A). Microscopy images taken after 1-hour exposure to 10 $\mu\text{g}/\text{mL}$ ticagrelor showed aggregates of BODIPY FL-vancomycin distributed within the bacterial cell (Fig. S3A and B), implying lipid II displacement and disturbed peptidoglycan synthesis machinery. Also, the rod-shaped bacteria became shorter and thicker, and cell curvature increased (Fig. S3C through E). Sub-inhibitory concentrations of ticagrelor, therefore, alter both *B. subtilis* and MRSA membrane properties in multiple ways.

Ticagrelor disrupts the integrity of the cytoplasmic membrane of Gram-positive bacteria

At the MIC (20 $\mu\text{g}/\text{mL}$), ticagrelor imposed changes that are characteristics of membrane-active agents in *B. subtilis* (18–22), including the formation of dye aggregates in the membrane (Fig. 3A and B), increased DAPI uptake (Fig. 3A and C), DNA condensation (Fig. 3A and D), and reduced cell length (Fig. 3A and E). The incorporation of the membrane-impermeant dye propidium iodide (PI) into the cytoplasm of *B. subtilis* indicated a breach of the cytoplasmic membrane barrier (Fig. 3F and G). A concentration and time-resolved study (Fig. S4) showed that below the MIC (10 $\mu\text{g}/\text{mL}$), PI could enter only a small fraction

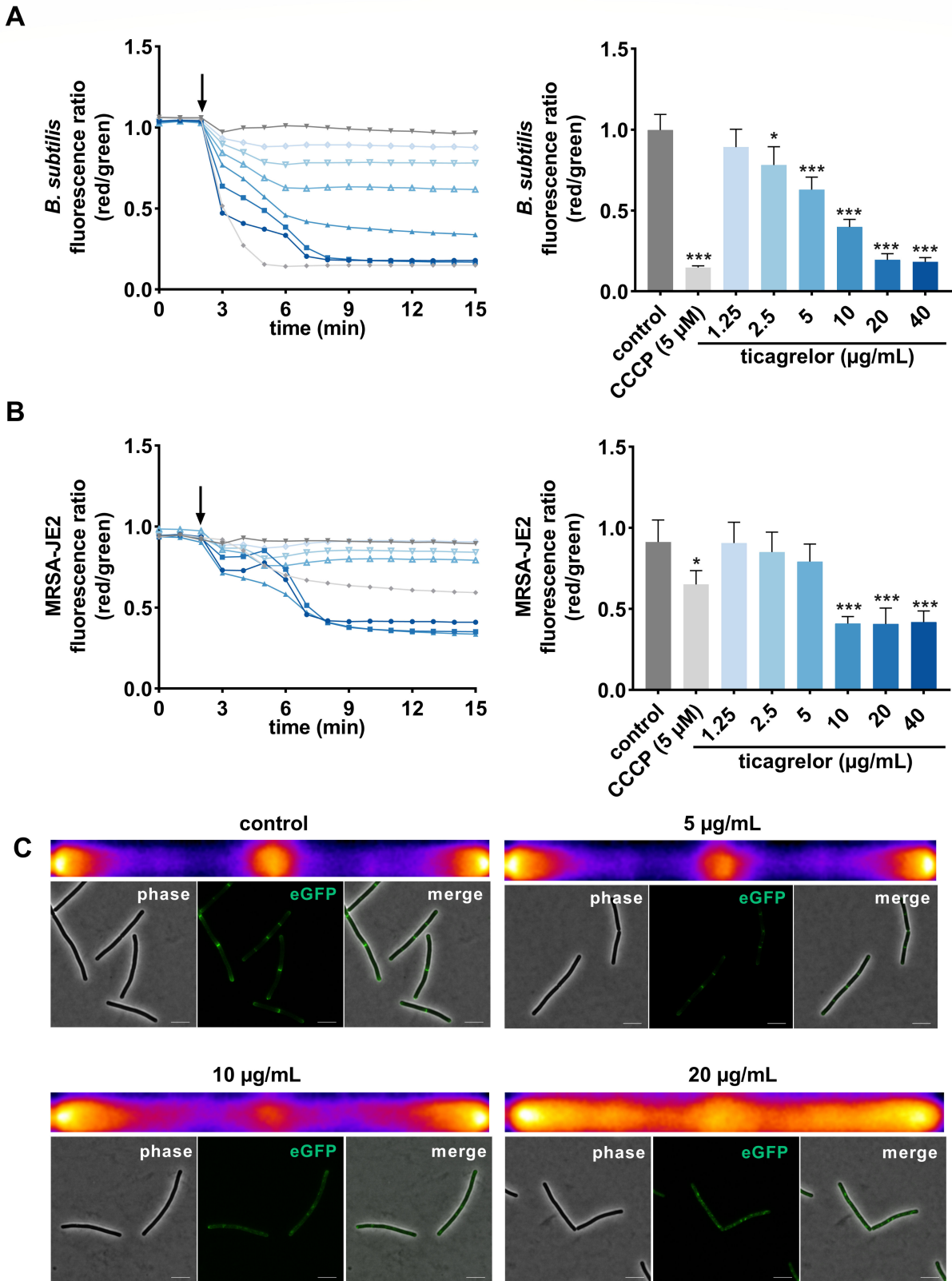


FIG 2 Ticagrelor dissipated the membrane potential of *Bacillus subtilis* and MRSA. Membrane potential over a period of 15 min, based on DiOC₂(3) staining, expressed as fluorescence ratio (red/green) with the addition (after 2 min, black arrow) of ticagrelor from 1.25 µg/mL to 40 µg/mL for *B. subtilis* 168 (N = 3), MRSA USA300 JE2 (N = 4), and MSSA (NCTC 8325), with CCCP (5 µM) as a positive control. (A) Quantitative analysis of the fluorescence ratio at 6 min after the (Continued on next page)

Fig 2 (Continued)

addition of compounds on *B. subtilis* 168 ($N = 3$), (B) *S. aureus* USA300 JE2 ($N = 4$). Graphs show mean \pm SD with control (1% DMSO). P -values were obtained via ANOVA using Dunnett's multiple comparison test compared to control, with $*P < 0.05$, and $***P < 0.001$. (C) Ticagrelor disrupts the septal localization of MinD. High-resolution microscopy images and heat maps of *B. subtilis* GFP-MinD treated with different concentrations of ticagrelor: 5 $\mu\text{g}/\text{mL}$ to 20 $\mu\text{g}/\text{mL}$. Heat maps show the average GFP signal for control and ticagrelor-treated cells after 10 min. More than 100 cells were analyzed per condition. The accumulated positional fluorescence information from >100 *B. subtilis* cells was transposed into each heat map, the left and right margins represent the cell poles of the rod-shaped cells and the middle corresponds to the septal region. Warmer and brighter colors indicate stronger localization of the fluorescent protein in this position. Scale bar, 5 μm . DiOC2(3), diethyloxacarbocyanine iodide; CCCP, chlorophenyl hydrazine.

of cells (10%–15%). At the MIC, membrane integrity was lost in 40% of cells after 20 min and in almost all cells after 2 h of ticagrelor exposure (Fig. S4A through C). A time-lapse study using the membrane-impermeable dye SYTOX Green as an alternative readout (Fig. S4D) showed membrane disruption by ticagrelor MIC after 10 min, which was almost as rapid as with the pore-former nisin (10 $\mu\text{g}/\text{mL}$) (Movies S1 to S3). The formation of membrane aggregates and PI uptake were also observed at the MIC of ticagrelor in MRSA (BAA-1556) (Fig. 3H through J) and MRSE (Fig. S5). To determine whether ticagrelor can interact with and disrupt lipid membranes without any interaction with a protein component, we performed a calcein release assay using artificial staphylococcus-like phospholipid liposomes (60% phosphatidylglycerol, 25% cardiolipin, and 15% lysophosphatidylglycerol). This assay showed concentration-dependent calcein release, starting at 10 $\mu\text{g}/\text{mL}$, with 20 $\mu\text{g}/\text{mL}$ ticagrelor causing complete disintegration of the liposome (Fig. 3K). Altogether, these data indicate that ticagrelor can rapidly kill Gram-positive bacteria, including MRSA and MRSE by disrupting the cytoplasmic membrane.

Ticagrelor targets multiple lipids in MRSA

To identify a molecular target of ticagrelor in Gram-positive bacteria, most particularly in MRSA, ticagrelor-resistant MRSA clones were selected *in vitro* using a gradient diffusion method. Nine clones resistant to the highest concentration of ticagrelor (>80 $\mu\text{g}/\text{mL}$) were selected for whole-genome sequencing. Eight clones displayed missense mutations in the *yjbH*, *clpX*, or *clpP* genes, and one clone had an insertion mutation (position 562) in the *yjbK* gene (locus tag USA300_FPR3757 SAUSA300_RS04870), encoding for a hypothetical protein (UniProt A0A2S6D7Y3). ClpX and ClpP are the substrate recognition subunits and the proteolytic subunit of the ClpXP protease, respectively, while YjbH is an adaptor protein that targets specific substrate proteins for degradation by bacterial ClpXP (23–25). All mutations in *yjbH* introduced a premature stop codon (amino acids 72, 97, and twice 105), one clone had a mutation in the *clpP* gene (Gly47Val), while the mutations in the *clpX* gene replaced amino acid Gly266 with Val in two clones, and with Cys in one clone. Of note, Gly266 localizes in the IGF motif required for ClpX-ClpP interaction, and substitutions in this motif are known to abolish ClpXP activity in *S. aureus* (24). We selected three different resistance mutations for further analysis, namely the *yjbH* Gln105stop, the *clpX* Gly266Val, and *clpP* Gly74Val. We verified that these mutated MRSA clones were resistant to ticagrelor as shown by normal growth in the presence of ticagrelor MIC (Fig. 4A). Under our *in vitro* growth conditions, growth rates of these three clones were similar to the MRSA parent strain (Fig. S6A). Since no molecular link has been established between the *S. aureus* ClpXP-YjbH protease and the bacterial membrane that we could have directly followed as a lead to the target of ticagrelor, we decided to obtain, as a next step, more insight into the general membrane composition of ticagrelor-resistant *S. aureus*. We performed a high-throughput lipidomic analysis to study changes in lipid composition in ticagrelor-resistant clones and identify possible lipid targets. These experiments made use of both exponential and stationary phase MRSA, characterized by well-known differences in lipid content (26, 27) (Fig. 4B through E; Table S1). Thirteen lipid classes and 97 lipid species were identified in the three mutated clones and the parent MRSA strain. Among the most abundant lipids, these analyses revealed an increased total content of phosphatidylglycerols (PG) in all

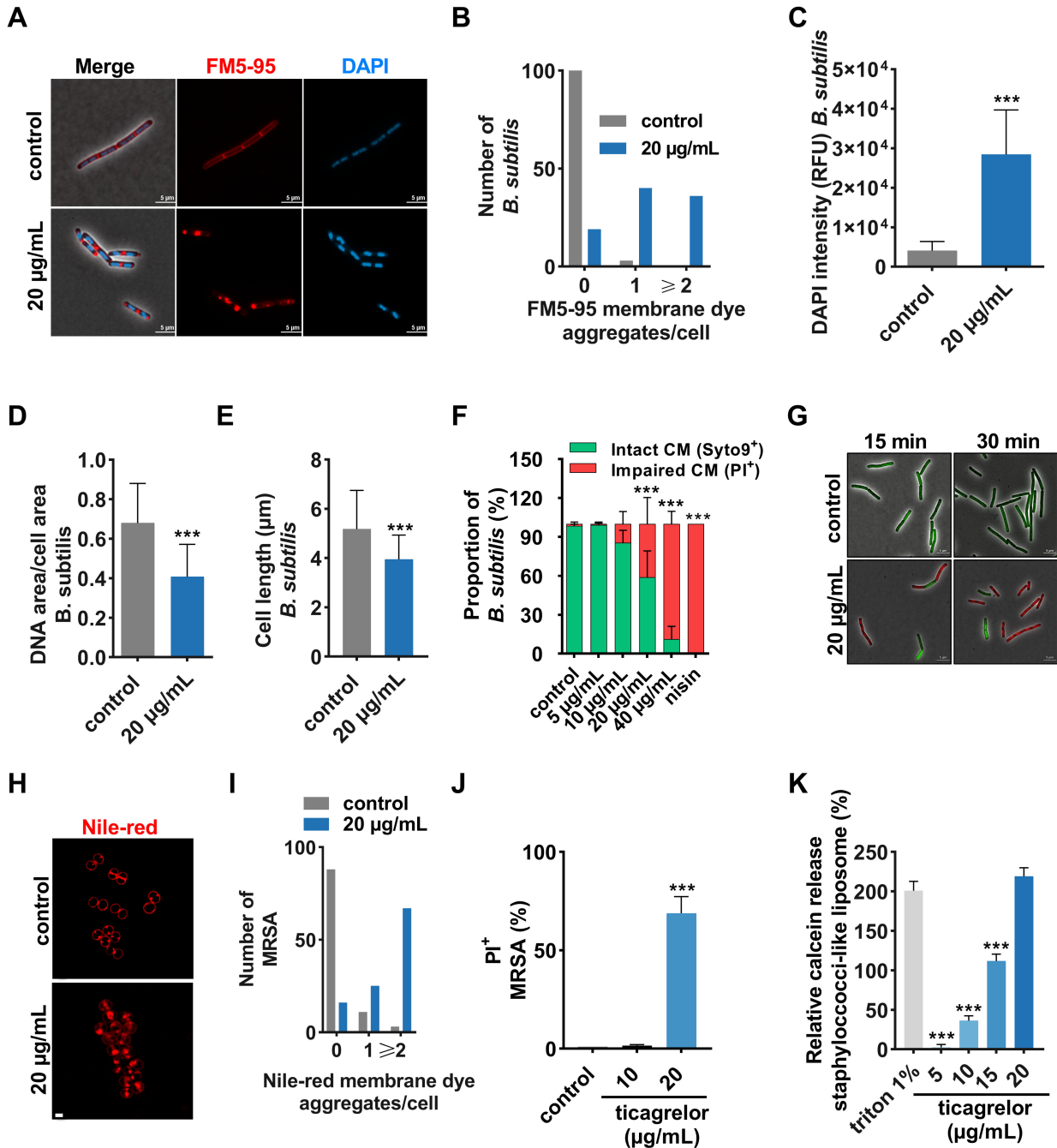


FIG 3 Ticagrelor disrupts the cytoplasmic membrane at the MIC. (A) Representative super-resolution microscopy images of *B. subtilis* 168 stained with FM5-95 and DAPI after 15-min treatment with 20 µg/mL ticagrelor (MIC concentration) compared to control, scale bar = 5 µm. Quantification of more than 100 *B. subtilis* cells from three biological replicates: (B) FM5-95 aggregates per cell shown as a histogram (Fisher exact test [$P < 0.001$]), (C) DAPI permeability, (D) DNA condensation, and (E) cell length. Graphs show mean \pm SD compared to control (1% DMSO). P -values were obtained via a t -test with $***P < 0.001$. (F) Quantification and (G) microscopy images of PI-positive *B. subtilis* assayed by PI and SYTO9 incorporation after 15 min of treatment with 10 µg/mL to 40 µg/mL ticagrelor compared to 10 µg/mL nisin, more than 100 cells were analyzed. (H) Representative super-resolution microscopy images of MRSA BAA-1556 stained with Nile-red after 1-hour treatment with 20 µg/mL ticagrelor compared to control, scale bar = 1 µm. (I) Quantification of Nile-red MRSA BAA-1556 membrane aggregates after treatment with 20 µg/mL ticagrelor of more than 100 cells, shown as a histogram (Fisher exact test; $P < 0.001$). (J) Quantification of PI-positive MRSA BAA-1556 using FACS after treatment with 10 µg/mL or 20 µg/mL of ticagrelor ($N = 4$). Graphs show mean \pm SD with control (1% DMSO). P -values were obtained via ANOVA using Dunnett's multiple comparison test compared to control (1% DMSO), with $***P < 0.001$. (K) Relative calcein release from calcein-encapsulated unilamellar *Staphylococcus*-like liposomes (60% PG, 25% CL, and 15% LPG) following treatment with ticagrelor from 5 µg/mL to 20 µg/mL, triton 1% was used as positive control. Graphs show mean \pm SD with control (1% DMSO). P -values were obtained via ANOVA using Dunnett's multiple comparison test compared to 1% triton, with $*P < 0.05$, $**P < 0.01$, and $***P < 0.001$. PI, propidium iodide; FACS, fluorescence-activated cell sorting.

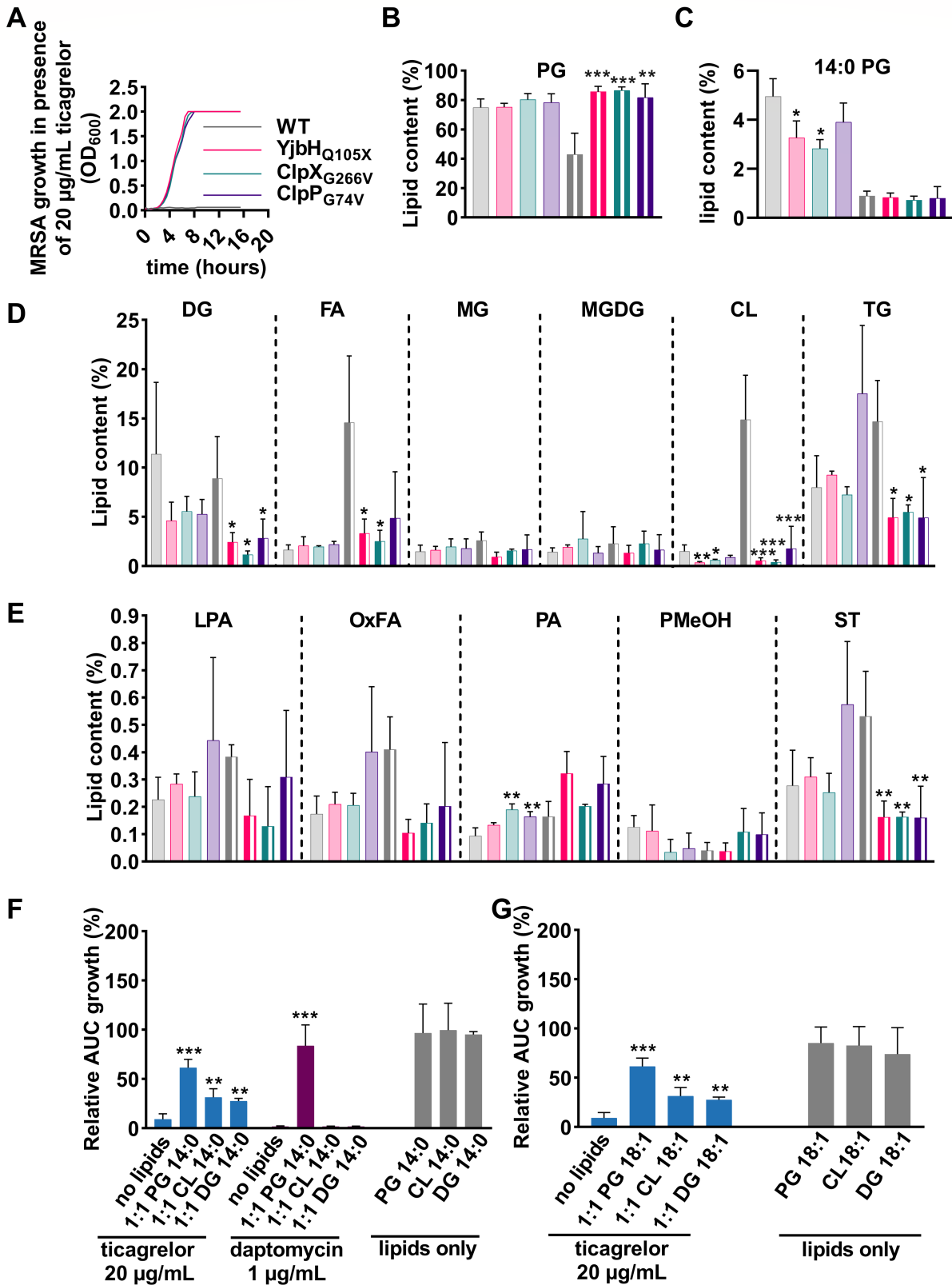


FIG 4 Ticagrelor targets multiple lipids in MRSA. (A) Bacterial growth curve of wild-type BAA-1556, YjbH_{Q105X}, ClpP_{G74V}, or ClpX_{G266V} in the presence of 20 µg/mL ticagrelor (*N* = 3). (B–E) Comparative lipidomic analysis of MRSA BAA-1556 WT compared to ticagrelor-resistant clones: YjbH_{Q105X}, ClpP_{G74V}, and ClpX_{G266V} (*N* = 3). Data are normalized to total lipid content or 14:0 fatty acyl chain-bearing PG, expressed as % lipid content showing exponential (full bar) (Continued on next page)

Fig 4 (Continued)

and stationary phase (striped pattern) bacteria. (F) Growth of MRSA BAA-1556 in the presence of 1:1 drug:lipid molar ratio for 20 $\mu\text{g}/\text{mL}$ ticagrelor or 1 $\mu\text{g}/\text{mL}$ daptomycin and 14:0 fatty acyl chain-bearing PG, CL, or DG with relative AUC growth (%) ($N = 4$). (G) Growth of MRSA BAA-1556 in the presence of 1:1 drug:lipid molar ratio for 20 $\mu\text{g}/\text{mL}$ ticagrelor and 18:1 fatty acyl chain-bearing PG, CL, or DG with relative AUC growth (%) ($N = 4$). Graphs represent mean \pm SD. P -values were obtained via ANOVA using Dunnett's multiple comparison test compared to WT or treatment without lipids with $*P < 0.05$, $**P < 0.01$, and $***P < 0.001$. AUC, area under the curve; PG, phosphatidylglycerol; DG, diacylglycerol; FA, fatty acids; MG, monoglycerides; MGDG, monogalactosyldiacylglycerol; CL, cardiolipin; TG, triglycerides; LTA, lysophosphatidic acid; OxFA, oxidized fatty acid; PA, phosphatidic acids; PMeOH, phosphatidyl methanol; ST, sterols; WT, and wild type.

stationary phase YjbH (Gln105X), ClpP (Gly266Val), and ClpX (Gly74Val) clones compared to parent MRSA, whereas the levels of cardiolipins (CL), diacylglycerols (DG), triglycerides (TG), and free fatty acids (FA) (two clones out of three) were significantly decreased. CL and 14:0 fatty acyl chain-bearing PG levels were also lower in exponential phase YjbH and ClpX mutants compared to the parent strain (Fig. 4C). In addition, we observed some changes in less abundant lipids, including sterol lipids (ST) that were reduced in all stationary phase mutants, and phosphatidic acid (PA) that was elevated in exponential phase ClpP and ClpX mutants as compared to parent MRSA. These findings indicate major modifications in the lipid composition of ticagrelor-resistant mutants, highlighting potential ticagrelor lipid targets.

Based on this data, a competitive quenching experiment was performed to assess the effect of exogenous lipids, including saturated short fatty acyl chain 14:0 and long 18:0, and mono-unsaturated 18:1 PG, CL, or DG, on the inhibition of bacterial growth by ticagrelor. We first verified that none of the tested lipids affected bacterial growth by themselves (Fig. 4F and G; Fig. S6F through H). All 14:0 and 18:1 lipids tested (PG, CL, and DG) inhibited the antibacterial properties of ticagrelor against MRSA at a 1:1 drug:lipid molar ratio (Fig. 4F and G; Fig. S6B and D), while the 18:0 variants failed to restore growth (Fig. S6E). In contrast to ticagrelor, daptomycin was only antagonized by PG lipids, as shown for 14:0 lipids (Fig. 4F; Fig. S6C). In accordance with these results, external lipids also antagonized the antibacterial activity of ticagrelor on *B. subtilis* (Fig. S7). Growth was fully restored at a drug:lipid molar ratio of 1:1 for CL and 1:2 for PG when 18:1 acyl chain lipids were used. DG had only a minor effect on *B. subtilis*. Similarly, as on MRSA, the 18:0 variants failed to restore growth of *B. subtilis*. These results uncover interactions between ticagrelor and multiple lipids of the bacterial cytoplasmic membrane.

Absence of cross-resistance between ticagrelor and daptomycin, or vancomycin

In view of our findings that ticagrelor has multiple targets in the bacterial membrane, we wanted to assess whether ticagrelor could retain activity against daptomycin-resistant *S. aureus*. A major resistance determinant for daptomycin reported in *S. aureus* is the spontaneous, and commonly observed, acquisition of gain-of-function mutations in the LysPG synthase/flippase MprF. We tested the *in vitro* and *in vivo* selected spontaneous mutations Thr345Ala and Val351Glu in MprF, expressed on a plasmid in the defined background of reference strain *S. aureus* 113 (28), as well as the daptomycin-resistant clinical isolates *S. aureus* 701 and 703, occurring in a patient under daptomycin therapy and both bearing a Ser295Leu MprF variant (29). While the strains showed up to 10-fold elevated MICs for daptomycin, their susceptibility against ticagrelor remained unchanged (Table 1). In addition, an *mprF* deletion mutant of *S. aureus* 113 showed a 13-fold higher susceptibility to daptomycin, while the MIC for ticagrelor was unaffected. In accordance with previous studies, the daptomycin-resistant mutants showed slightly reduced susceptibility to vancomycin (28, 29). Moreover, the ticagrelor MIC against vancomycin-intermediate *Staphylococcus aureus* (VISA) strain Mu50 remained at 20 $\mu\text{g}/\text{mL}$ of ticagrelor (Table 1). Furthermore, the ticagrelor-resistant mutants YjbH (Gln105stop), ClpP (Gly74Val), and ClpX (Gly266Val) were equally susceptible to daptomycin and vancomycin, as was the MRSA parent strain BAA-1556. The susceptibility

TABLE 1 MIC determination of ticagrelor, daptomycin, or vancomycin against daptomycin (MprF)-, ticagrelor (YjbHQ_{105X}, ClpX_{G266V}, and ClpP_{G74V})- or vancomycin (VISA Mu50)-resistant strains

		MIC ^a (μg/mL)		
		Ticagrelor	Daptomycin	Vancomycin
<i>S. aureus</i> SA113	WT	20 (20/20/20)	2 (2/2/2)	1 (1/1/1)
	ΔMprF	26.7 (40/20/20)	0.2 (0.3/0.1/.1)	0.5 (0.5/0.5/.5)
	MprF _{T345A}	20 (20/20/20)	9.3 (8/16/4)	1.3 (1/1/2)
	MprF _{V351E}	20 (20/20/20)	5.3 (4/8/4)	1.7 (2/1/2)
Clinical isolates	WT (616)	20 (20/20/20)	0.8 (1/1/.5)	1 (1/1/1)
<i>S. aureus</i>	MprF ₇₀₁	20 (20/20/20)	10.7 (8/16/8)	2.7 (2/2/4)
	MprF ₇₀₃	20 (20/20/20)	10.7 (8/16/8)	1.7 (1/2/2)
MRSA	WT	20 (20/20/20)	0.7 (1/0.5/.5)	1 (1/1/1)
BAA-1556	YjbHG _{105X}	>80 (>80/>80/>80)	0.8 (1/1/.5)	1 (1/1/1)
	ClpX _{266V}	>80 (>80/>80/>80)	0.8 (1/0.5/1)	1 (1/1/1)
	ClpP _{G74V}	>80 (>80/>80/>80)	1 (1/1/1)	1 (1/1/1)
VISA Mu50	WT	20 (20/20/20)	2 (2/2/2)	5 (8/4/4)

^aMean of three biological replicates, with individual values obtained in three independent repetitions shown in parentheses.

of ticagrelor-resistant mutants to daptomycin and vancomycin was further confirmed in a time-kill assay, which showed identical bactericidal activity of daptomycin (20 μg/mL) and vancomycin (10 μg/mL) on the MRSA parent strain and the ticagrelor-resistant mutants (Fig. 5A and B). In addition, ticagrelor killed VISA and vancomycin-susceptible MRSA with the same efficacy (MBC = 20 μg/mL) (Fig. 5C) (8). Altogether, these data indicate no cross-resistance between ticagrelor and vancomycin or daptomycin.

Ticagrelor enhances the activity of daptomycin and vancomycin

We further investigated the interactions between ticagrelor, vancomycin, or daptomycin by combining the drugs two-by-two in checkerboard assays. A combination of a twofold dilution series ranging from 5 μg/mL to 40 μg/mL for ticagrelor and 0.25 μg/mL to 1 μg/mL for daptomycin or vancomycin showed an additive effect against MRSA BAA-1556 with a ΣFIC of 1.25 when combining ticagrelor with daptomycin and a ΣFIC of 1 for vancomycin (Fig. 6A and B). A twofold dilution series from 5 μg/mL to 40 μg/mL for ticagrelor and 0.25 μg/mL to 4 μg/mL for daptomycin also displayed an additive effect on VISA Mu50 with a ΣFIC of 1 (Fig. 6C). A similar additive effect was observed when measuring 5 μg/mL to 40 μg/mL ticagrelor in combination with 0.5 μg/mL to 16 μg/mL vancomycin against VISA Mu50 with a ΣFIC of 1.25 (Fig. 6D). We then assessed the capacity of ticagrelor by its own or in combination with daptomycin or vancomycin to kill stationary phase MRSA. The number of viable bacteria was determined over 5 days. Ticagrelor (up to 40 μg/mL) did not show any bactericidal effect on stationary phase MRSA (Fig. 6E and F). In agreement with previous studies (8, 30), these stationary bacteria were killed by 20 μg/mL daptomycin, which corresponds to its MBC on exponential phase MRSA (Fig. 6E). By contrast, vancomycin was inactive against stationary phase MRSA at the concentration effective against exponentially growing cells (10 μg/mL) (Fig. 6F). Interestingly, combining 40 μg/mL ticagrelor with 10 μg/mL vancomycin could kill stationary phase MRSA (Fig. 6F). In addition, a combination of 20 μg/mL (or 40 μg/mL) ticagrelor with sub-MBC of daptomycin (10 μg/mL) induced a transient decrease in viable bacteria (Fig. 6E). These results are therefore indicative of enhanced antibacterial activity of vancomycin and daptomycin in the presence of ticagrelor.

DISCUSSION

Here, we show that the antiplatelet drug ticagrelor alters the property and integrity of the cytoplasmic membrane of Gram-positive bacteria in a dose-dependent manner and through a unique mode of action. Notably, this drug retained activity against multi-drug-resistant *S. aureus*, including isolates carrying the most common *in vivo* selected

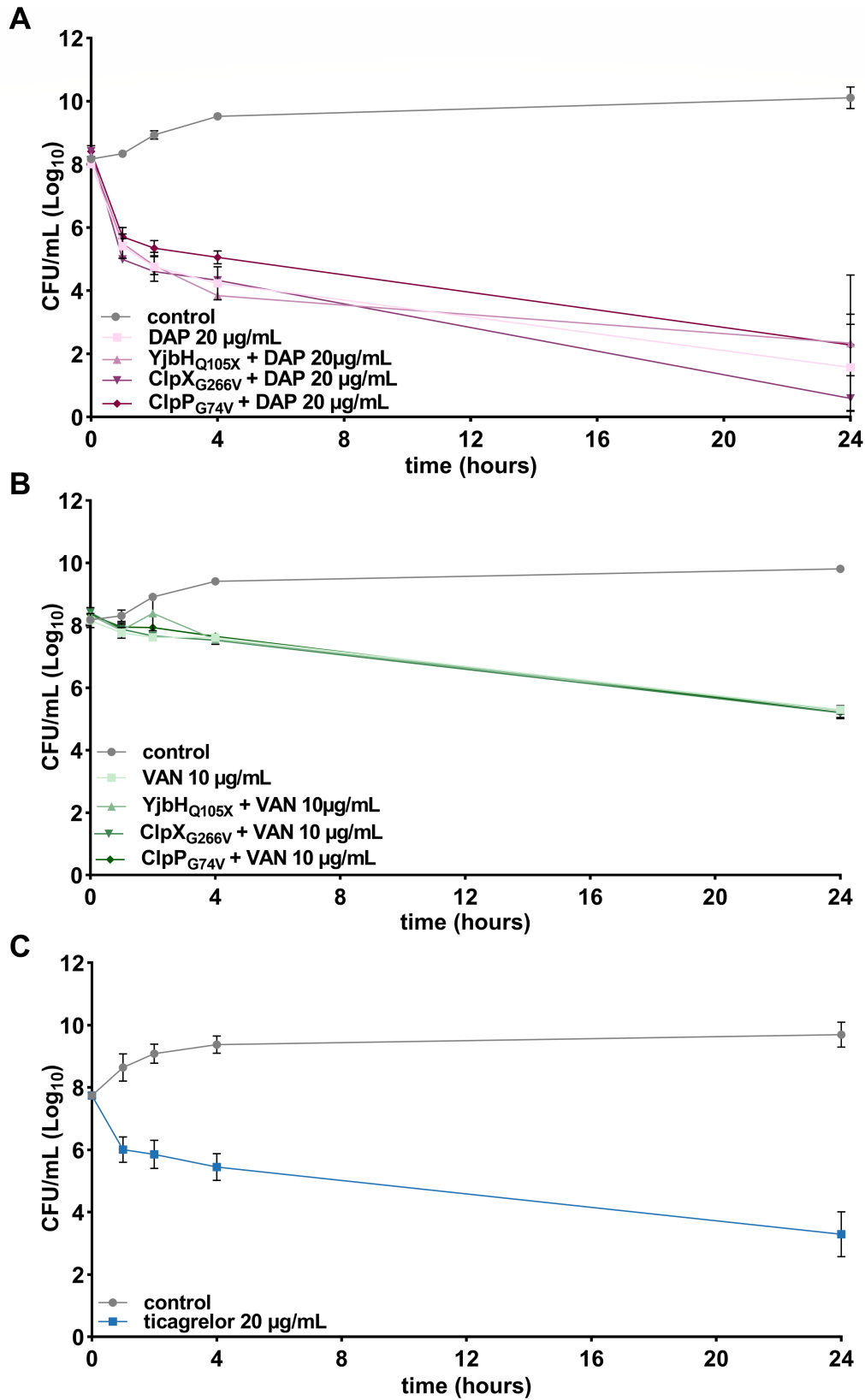


FIG 5 No cross-resistance between daptomycin, vancomycin, and ticagrelor. Time-kill assay of wild-type MRSA BAA-1556 and ticagrelor-resistant clones (YjbH_{Q105X}, ClpX_{G266V}, and ClpP_{G74V}) in the presence of (A) 20 µg/mL daptomycin or (B) 10 µg/mL vancomycin and (C) VISA Mu-50 in the presence of 20 µg/mL ticagrelor. Graphs represent mean ± SD of log₁₀ CFU/mL at 0, 1, 2, 4, and 24 hours with control representing 1% DMSO treatment of wild type (N = 3). VISA, vancomycin-intermediate *Staphylococcus aureus*; DAP, daptomycin; VAN, vancomycin.

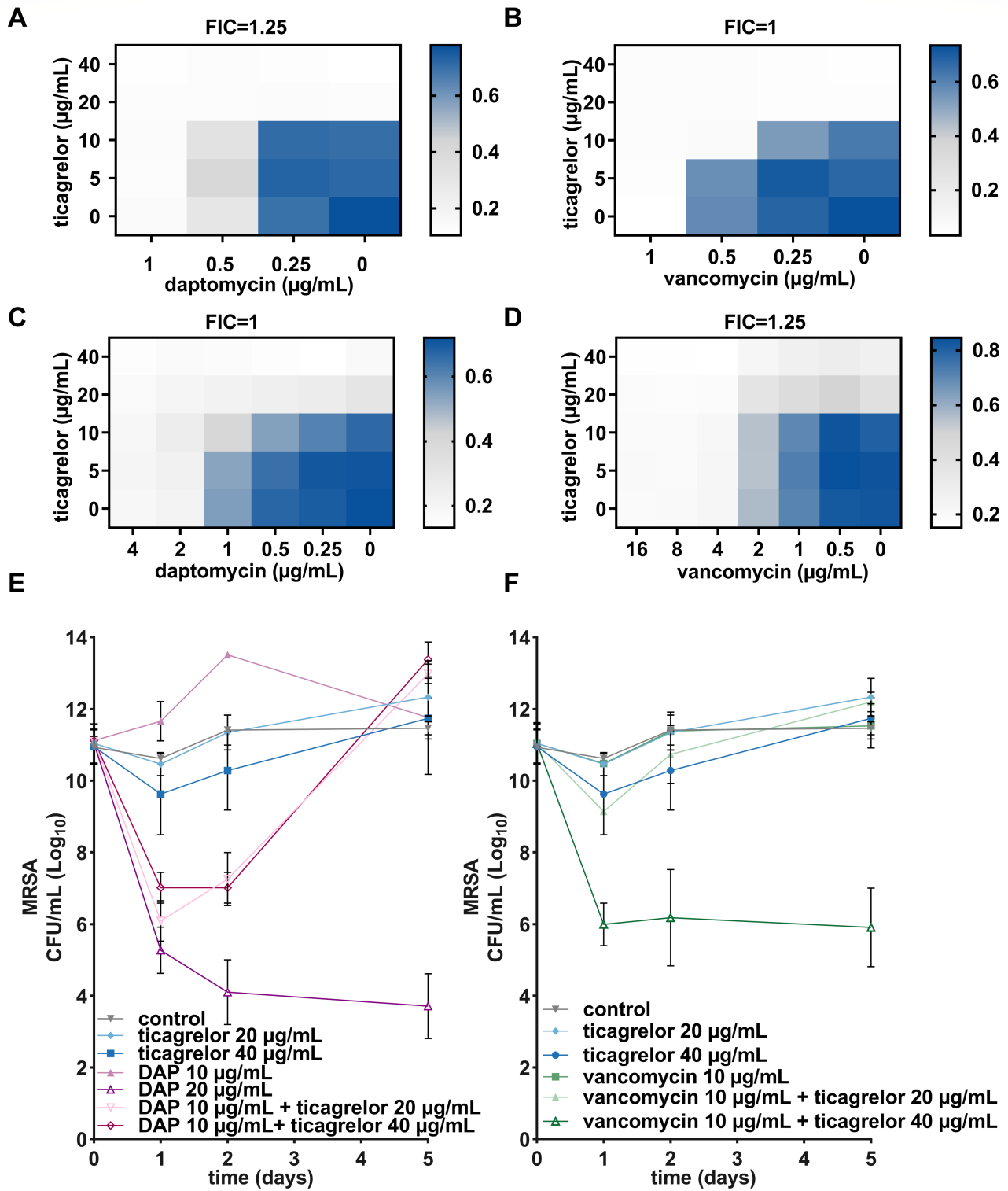


FIG 6 Ticagrelor enhances the activity of daptomycin and vancomycin. Checkerboard assay using MRSA BAA-1556 with a twofold dilution series of (A) ticagrelor from 40 µg/mL to 5 µg/mL (vertical) and daptomycin from 1 µg/mL to 0.25 µg/mL ($N = 5$), or (B) vancomycin from 1 µg/mL to 0.25 µg/mL (horizontal) ($N = 3$), and (C) VISA with a twofold dilution series of ticagrelor from 40 µg/mL to 5 µg/mL (vertical), daptomycin from 4 µg/mL to 0.25 µg/mL (horizontal) ($N = 6$) or (D) VISA with a twofold dilution series of ticagrelor from 40 µg/mL to 5 µg/mL (vertical), and vancomycin from 16 µg/mL to 0.5 µg/mL (horizontal) ($N = 6$). Data are represented as a heat map with mean values of ΔOD_{600} determined as the difference in OD_{600} at timepoint 0 and after 24 hours treatment. (E and F) Bacterial killing of stationary phase MRSA BAA-1556 by a combination of 20 µg/mL or 40 µg/mL ticagrelor with 10 µg/mL daptomycin or 10 µg/mL vancomycin ($N = 3$). Graphs represent mean \pm SD of log₁₀ CFU/mL over a period of 5 days with control being 1% DMSO treatment of wild type. VISA, vancomycin-intermediate *Staphylococcus aureus*; DAP, daptomycin; VAN, vancomycin.

daptomycin-resistant mechanism and VISA. We also found that the activity of daptomycin and vancomycin against MRSA was increased in the presence of ticagrelor. Our findings are of clinical importance since these antibiotics are conventionally used to treat MRSA-induced infections and are further relevant considering expanding vancomycin resistance (31).

Similarly to daptomycin and vancomycin, ticagrelor induced bacterial cell envelope stress biomarkers in *B. subtilis* bioreporter strains, pointing to an effect on the bacterial membrane or cell wall (13, 32). Ticagrelor triggered several dose-dependent effects on bacterial membranes that are reminiscent of membrane-active agents (33, 34), including membrane depolarization, the formation of membrane dye aggregates, DNA condensation, and an increased uptake of DAPI and membrane impermeant dyes. Delocalization of the peptidoglycan precursor lipid II and of the cell division regulator MinD, along with changes in cell morphology indicated extensive disturbance of membrane topology, culminating in the loss of membrane integrity allowing dye molecules to enter the cell. Ticagrelor-induced disruption of the bacterial cytoplasmic membrane was demonstrated in several Gram-positive strains, including *B. subtilis*, MRSA, and MRSE. We further confirmed a direct effect of ticagrelor on the integrity of a phospholipid bilayer using staphylococci-like artificial liposomes in a calcein release assay.

The cell wall is the first structure that ticagrelor must pass before reaching the cytoplasmic membrane. In this work, apart from a rearrangement of the lipid II precursor involved in peptidoglycan synthesis by ticagrelor, we did not investigate potential direct interactions of ticagrelor with cell wall components or specific impairment of cell wall biosynthetic reactions. Using thermal proteome profiling, a recent study described that ticagrelor destabilized a subunit of the cell wall teichoic acid translocase in live cells, and two proteins involved in the lipoteichoic acid D-alanylation in cell lysates (35). Impairment of these enzyme activities would increase the net negative charge of *S. aureus* surface, which would result in the observed susceptibility of ticagrelor-treated bacteria to cationic antibiotics such as aminoglycosides and nisin (35). Further investigations might be warranted to characterize the surface polarity and charge of *S. aureus* considering different ticagrelor concentrations, durations of treatment and environmental conditions.

To identify a potential target of ticagrelor, we generated ticagrelor-resistant MRSA clones *in vitro*. Eight of the nine generated clones showed mutations in the *clpP*, *clpX*, or *yjbH* gene. Although no molecular link has been established yet between the ClpXP protease complex and the bacterial membrane, protein degradation through this complex is crucial in controlling stress responses, virulence, and biofilm formation (24, 36–38). *S. aureus* strains with loss of function mutations in ClpXP components are more resistant to certain types of antibiotic stress and show reduced virulence (30, 37, 39). Because these strains are potentially non-infectious, the loss of function mutants have a low occurrence *in vivo*. Interestingly, we previously described that ticagrelor reduces virulence factor expression with a downregulation of several *agr* components (9). While the ClpXP protease has pleiotropic cellular roles, the YjbH adaptor protein specifically targets the transcriptional stress regulator Spx for degradation by the ClpXP protease (23, 36, 40). Inactivation of YjbH prevents Spx from being degraded by the ClpXP protease and is of high relevance, we recently found that high Spx broadly promoted the growth of MRSA in the presence of compounds targeting the cell wall or the cell membrane, including the membrane-specific pore-former nisin (41). Understanding the link between ticagrelor activity or resistance in relation to the ClpXP-YjbH complex will require further investigation, however, increased Spx levels, as a consequence of out-of-function mutations in ClpP, ClpX, or YjbH, are one plausible explanation for the decreased sensitivity of *S. aureus* to ticagrelor.

Preliminary data (not shown) do not indicate that ClpP, ClpX, or YjbH are direct targets of ticagrelor. Instead, the modified lipid composition of generated ticagrelor-resistant clones along with our antibacterial activity antagonizing assays in the presence of exogenous lipids revealed lipid targets for ticagrelor. Among the most abundant lipids

in *S. aureus*, we observed lower levels of CL, DG, TG, and FA as well as of 14:0 fatty acyl chain-bearing PG in ticagrelor-resistant clones. Accordingly, our antagonizing assays revealed that PG, CL, and DG restored bacterial growth. Interestingly, we noted a strong influence of the fatty acid side chains, with shorter (14:0) or unsaturated, long (18:1) fatty acids rescuing bacterial growth more strongly than saturated, long acyl chains (18:0), which may imply that lipid fluidity is required for the protective effect. Our data rule out general interactions of ticagrelor with all amphipathic lipids. However, the exact mechanisms underlying ticagrelor-lipid interactions remain to be determined.

In contrast to ticagrelor which showed interactions with multiple lipids, our antagonizing assays indicated that daptomycin is preferentially bound to PG, as compared to CL and DG. Daptomycin is a Ca^{2+} -dependent cyclic lipopeptide that is highly potent against MRSA. According to the current model, after binding calcium, Ca^{2+} -daptomycin forms a tripartite complex with PG and undecaprenyl-coupled peptidoglycan precursors in *S. aureus* membranes. While, initially, daptomycin binding occurs primarily at the septum affecting peptidoglycan synthesis, major membrane rearrangements follow, resulting in lipid clustering, detachment of peripheral membrane, and gradual membrane disintegration (42–46). Importantly, ticagrelor remained active against daptomycin resistance mutations in MprF, which are commonly selected *in vivo* (28, 29, 47, 48). Recent advances showed that most point mutations in MprF causing daptomycin resistance cumulate in a hot spot region of the MprF flippase part (e.g., T345A, V351E) (28). Since intramolecular domain interactions in the MprF flippase are weakened in these mutants, the authors suggested a mechanistic model in which daptomycin can directly be bound and expelled from the cell by MprF (28). This mechanism is strongly supported by the recently presented cryo-electron microscopy structure of MprF and a computational docking study suggesting that daptomycin can fit well in the active flippase region when above-mentioned point mutations are introduced (49). Therefore, most *S. aureus* resistance mechanisms to daptomycin appear to be tailored to its structure and, in agreement with our data, do not affect ticagrelor sensitivity. *Vice versa*, ticagrelor-resistant strains bearing YjbH_{Q105X}, ClpP_{G74V}, and ClpX_{G266V} mutations remained sensitive to daptomycin. Besides daptomycin, vancomycin is an antibiotic that is broadly and conventionally used to treat MRSA infections (50). Here, the well-characterized VISA Mu-50 strain was sensitive to ticagrelor, and vancomycin remained active against all ticagrelor-resistant MRSA clones. Our data therefore support the ability of ticagrelor to circumvent these traditional antibiotic resistance mechanisms, thereby offering a potential alternative treatment option for difficult-to-treat infections. In addition, our data indicated that ticagrelor increased the antibacterial activity of daptomycin and vancomycin against MRSA and VISA. When combined with vancomycin, ticagrelor could even kill MRSA in the stationary phase, while the drugs had no effect on their own. Despite additive potential, standard checkerboard assays showed no synergistic effects between ticagrelor and daptomycin or vancomycin, further supporting distinct mechanisms of action. In line with our observations, an additive effect of ticagrelor together with vancomycin was previously reported against *C. difficile* (7).

In conclusion, our study shows that ticagrelor targets major lipids in the Gram-positive bacteria membrane and causes dose-dependent membrane alterations and disruption while retaining activity against multidrug-resistant staphylococci including daptomycin- and vancomycin-resistant strains.

MATERIALS AND METHODS

Additional materials and methods are described in the supplemental material.

Bacterial strains and growth conditions

The bacterial strains used in this study are listed in Table S2. Bacteria were aerobically cultured at 37°C under continuous shaking (200 rpm) in indicated media.

Bioreporter assays

The *B. subtilis* 1534 *luc* bioreporter strains using the firefly luciferase as readout were generated and validated by Urban and colleagues (13). The method was adjusted as follows: Overnight cultures of *B. subtilis* P_{yypuA} , P_{lial} , P_{yorB} , P_{helD} , and P_{bmrC} -*luc* were diluted to an OD₆₀₀ of 0.05 in lysogeny broth (LB) medium and incubated at 37°C at 190 rpm until an OD₆₀₀ of 0.9 was reached. Bacteria were then diluted in LB medium (P_{yypuA} , P_{lial} , P_{yorB} , and P_{helD}) or Belitzky (51) minimal medium (P_{bmrC}) to an OD₆₀₀ of 0.02 and further diluted 1:1 to medium containing a twofold serial dilution from 80 µg/mL to 0.08 µg/mL for ticagrelor, 12.5 µg/mL to 0.01 µg/mL for vancomycin, 6.25 µg/mL to 0.003 µg/mL for ciprofloxacin, 0.006 µg/mL to 0.000003 µg/mL for rifampicin, 25 µg/mL to 0.01 µg/mL for chloramphenicol, or 32 µg/mL to 0.04 µg/mL for daptomycin and incubated at 37°C for 1 hour in a white flat-bottom 96-well plate. Luminescence was measured in a Tecan SPARK reader 5 seconds after adding 0.1 M citrate buffer (pH 5) containing 2 mM luciferin. The agar-based bioreporter assay method is described in the supplemental material.

Membrane potential assay

Bacterial cultures were grown in LB medium to an OD₆₀₀ of 0.75. Bacteria were pelleted and resuspended to an OD₆₀₀ of 0.5 in phosphate-buffered saline (PBS) and incubated with 30 µM 3,3'-diethylthiocarbocyanine iodide [DiOC2(3)] for 15 minutes in the dark. Cells were transferred to a black 96-well flat-bottom polystyrene microtiter plate and baseline fluorescence was recorded for 2 minutes. Next, a concentration series of ticagrelor was added and fluorescence was measured for a total of 15 minutes using a spectrophotometer (TECAN Spark) with λ_{ex} of 485 nm and λ_{em} of 530 nm and 630 nm. The protonophore CCCP (5 µM) was used as a positive control.

Microscopic phenotyping

B. subtilis 168 trpC2 cultures were grown in LB medium to an OD₆₀₀ of 0.25 and treated with ticagrelor at the indicated concentrations. *B. subtilis* microscopic phenotyping was performed according to previously described methods (see the supplemental material). For MRSA (BAA-1556) and MRSE, overnight bacterial cultures were grown in a TSB medium followed by treatment with ticagrelor. After 1 hour, MRSA was stained for 5 minutes at 37°C with 5 µg/mL Nile-red. After staining, cells were placed in a Gene Frame (ThermoFisher Scientific) on an agarose pad and imaged using a Zeiss Elyra 7 microscope. Propidium iodide (PI) incorporation by MRSA was analyzed after the addition of 1 µg/mL PI. MRSE PI incorporation was determined via flow cytometry, bacteria were stained with 0.1 mg/mL PI for 5 minutes at 37°C, and PI uptake was recorded using a Cytoflex flow cytometer (Beckman Coulter).

Calcein-loaded liposomes

Calcein solution (60 mM) was prepared in 5 mM HEPES, pH 7.4. Staphylococcus-like liposomes were composed of lysyl-phosphatidylglycerol (LPG) (15%) (Lipoid S100 579000-1170722-10/919), phosphatidylglycerol (PG) (60%) (Avanti, 841188P), and cardiolipin (CL) (25%) (Avanti, 710335P). Lipids were solubilized in ethanol, mixed, and dried in a rotavapor at 30°C for 1 hour. The thin lipidic film was hydrated directly with the calcein solution and the dispersion was extruded three times per filter (three different sizes of filters were sequentially used 0.4 µm, 0.2 µm, and 0.14 µm). The liposome suspension was then washed four times by ultracentrifugation to remove free calcein (35,000 rpm, 4°C, 2 h). Calcein release was measured for 30 min at 37°C in 100 µL of a solution containing 10 mM HEPES pH 7.4 and NaCl 150 mM.

Minimal inhibitory concentration determination

The MIC of the test compounds was determined by standardized procedures according to the guidelines of EUCAST or CLSI.

Generation of ticagrelor-resistant mutants and whole-genome sequencing of resistant strains

Ticagrelor-resistant MRSA (BAA-1556) strains were obtained through a gradient diffusion method. The genomic DNA of nine generated ticagrelor-resistant clones was isolated from bacterial pellets using the High Pure kit (Roche, Life Science). Sequencing was carried out using MiSeq v2 kits following the manufacturer's standard protocols (Illumina Inc, USA). Sequencing was carried out using MiSeq v2 kits following the manufacturer's standard protocols (Illumina Inc, USA). Comparative genomics analysis was performed on the nine clones and wild-type MRSA. Fastq files of the isolated mutants were mapped against the MRSA reference genome (USA300_FPR3757). All genomes have been mapped using BWA. Prior to these mappings, the raw data from sequencing have been preprocessed using a pipeline based on BBTools (52). The following steps have been made in order: deduplication, adapter trimming, quality recalibration, error correction, and quality trimming with a minimum set of 8. The variant calling has been made using BBTools with a minimum coverage of 5, a minimum average quality of 15, and a minimum fraction of 75%.

Lipidomic analyses

MRSA wild-type (BAA-1556) and ticagrelor-resistant strains were grown in the TSB medium. Overnight bacterial cultures were diluted 100 times in fresh TSB and allowed to grow in the exponential phase or overnight until the stationary phase. Bacteria were collected by centrifugation at $14,000 \times g$ for 5 minutes and washed once in NaCl 0.9%. All values were normalized to the total amount of lipids and expressed as % of lipid content. Lipids were extracted using a modified MTBE protocol according to Matyash et al. (53). Untargeted lipidomic analysis was performed using an LC-MS/MS-based lipid profiling method as previously reported (54), except for the following parameters: ion source gas 1, 2 and curtain gas were 45, 50, and 35 psi, respectively, and an acquisition range of m/z 100–1,800 was applied. In addition, a CL-focused analysis was conducted by adjusting the untargeted lipidomics method so that enhanced MS/MS fragmentation could be obtained assisting CL identification. For this, the collision energy and collision energy spread parameters were set to -60 and -5 V, respectively.

Lipid-based antagonization assays

The effect of 14:0 PG (840445), -cardiolipin (750332), -DG (800814) and 18:1 PG (840521P), -cardiolipin (710335P), -DG (800811C) (Avanti lipids, Sigma-Aldrich) on the inhibition of bacterial growth by ticagrelor or daptomycin was assessed as follows. Overnight MRSA (BAA-1556) cultures were diluted 1,000 times in TSB medium and mixed with lipids at a 1:1 (drug:lipid) molar ratio. Bacterial growth (OD_{600}) was measured over time, and the area under the curve (AUC) was determined and expressed as relative AUC (%).

Time kill assay

Bacteria were grown in an MHB medium and treated with vehicle or test compounds. The number of live bacteria (CFU/mL) was determined over time.

Checkerboard assay

Checkerboard assays were performed in MHB medium (after the addition of $50 \mu\text{g/mL}$ Ca^{2+} for daptomycin) according to the standard procedures.

Data analysis

Statistical analyses were done using GraphPad Prism 9 software. A parametric *t*-test or ANOVA with Dunnett's multiple comparison was performed. Categorical data were analyzed via a Fisher exact test. Graphs represent mean \pm SD with *P* values: **P* < 0.05, ***P* < 0.01, and ****P* < 0.001.

ACKNOWLEDGMENTS

The authors thank the GIGA technological platforms, particularly GIGA-Genomics.

C.O. is a Research Director at the Belgium National Funds for Scientific Research (F.R.S.-FNRS). Research from the University of Liège (ULiège) is funded by F.R.S.-FNRS (grant number PDR T.0190.20) to C.O., ULiège internal Fund grant numbers FSR-S-SS-19/18 and FSR-S-SS-21/41 to C.O., and European Research Council Consolidator grant (grant number 647197) to P.L. S.M. has a fellowship from the FRIA (Belgium National Funds for Scientific Research). This work was supported by funding from the German Center for Infection Research, DZIF (D.C.S. and H.B.-O.) via project TTU 09.826 (PAACT), from the Deutsche Forschungsgemeinschaft (German Research Foundation, DFG) (L.A.E. and H.B.-O.) via TRR 261 (project ID 398967434). H.B.-O. and D.C.S. acknowledge infrastructural support from the Cluster of Excellence EXC 2124: Controlling Microbes to Fight Infection (CMFI, project ID 390838134) and L.A.E. from the Max-Planck Research School "From Molecules to Organisms," Tuebingen.

AUTHOR AFFILIATIONS

¹Laboratory of Cardiology, GIGA Research Institute, University of Liège, Liège, Belgium

²Department of Microbial Bioactive Compounds, Interfaculty Institute of Microbiology and Infection Medicine Tübingen (IMIT), University of Tübingen, Tübingen, Germany

³Department of Veterinary and Animal Sciences, Faculty of Health and Medical sciences, University of Copenhagen, Copenhagen, Denmark

⁴Leiden University Medical Center, Center for Proteomics and Metabolomics, Leiden, the Netherlands

⁵Laboratory of Pharmaceutical Technology and Biopharmacy, Nanomedicine Developments, Center for Interdisciplinary Research on Medicines (CIRM), University of Liège, Liège, Belgium

⁶Bacterial physiology and genetics–Centre d'Ingénierie des Protéines-Integrative Biological Sciences, Department of Life Sciences, University of Liège, Liège, Belgium

⁷Pediatric Surgery and Urology, University Children's Hospital Tübingen, University of Tübingen, Tübingen, Germany

⁸German Center for Infection Research (DZIF), Partner Site Tübingen, Tübingen, Germany

⁹Cluster of Excellence "Controlling Microbes to Fight Infections (CMFI)", University of Tübingen, Tübingen, Germany

¹⁰Laboratory of Medicinal Chemistry, Center for Interdisciplinary Research on Medicines (CIRM), University of Liège, CHU Sart Tilman, Liège, Belgium

AUTHOR ORCID*s*

Christoph J. Slavetinsky  <http://orcid.org/0000-0001-5576-5906>

Dorte Frees  <http://orcid.org/0000-0003-4946-2890>

Heike Brötz-Oesterhelt  <http://orcid.org/0000-0001-9364-1832>

Cécile Oury  <http://orcid.org/0000-0002-7561-0132>

FUNDING

Funder	Grant(s)	Author(s)
Fonds De La Recherche Scientifique - FNRS (FNRS)	PDR T.0190.20	Cécile Oury

Funder	Grant(s)	Author(s)
Fédération Wallonie-Bruxelles (French Community of Belgium)	FSR-S-SS-19/18, FSR-S-SS-21/41	Cécile Oury
EC European Research Council (ERC)	647197	Patrizio Lancellotti
Deutsches Zentrum für Infektionsforschung (DZIF)	TTU 09.826	Heike Brötz-Oesterhelt
Deutsche Forschungsgemeinschaft (DFG)	TRR 261 project 398967434	Heike Brötz-Oesterhelt

AUTHOR CONTRIBUTIONS

Kirsten Leeten, Conceptualization, Data curation, Formal analysis, Investigation, Methodology, Writing – original draft | Nicolas Jacques, Formal analysis, Investigation, Methodology | Lidia Alejo Esquembre, Formal analysis, Investigation, Methodology | Dana C. Schneider, Formal analysis, Investigation, Methodology | Jan Straetener, Data curation, Formal analysis, Investigation, Methodology | Camilla Henriksen, Data curation, Formal analysis, Methodology | Lucia Musumeci, Formal analysis, Investigation, Methodology | Florence Putters, Formal analysis, Investigation, Methodology | Sofia Melo, Formal analysis, Investigation, Methodology | Elena Sánchez-López, Data curation, Formal analysis, Investigation, Methodology | Martin Giera, Data curation, Formal analysis, Investigation, Methodology | Noémie Penoy, Data curation, Formal analysis, Methodology | Géraldine Piel, Data curation, Formal analysis, Methodology | Olivier Verlaine, Data curation, Formal analysis, Investigation, Methodology | Ana Amoroso, Data curation, Formal analysis, Investigation, Methodology | Bernard Joris, Data curation, Formal analysis, Investigation, Methodology | Christoph J. Slavetinsky, Data curation, Formal analysis, Resources | Eric Goffin, Formal analysis, Investigation, Methodology | Bernard Pirotte, Data curation, Formal analysis, Methodology, Resources | Dorte Frees, Conceptualization, Data curation, Formal analysis, Investigation, Methodology, Supervision, Writing – review and editing | Heike Brötz-Oesterhelt, Conceptualization, Data curation, Formal analysis, Funding acquisition, Investigation, Methodology, Supervision, Writing – review and editing | Patrizio Lancellotti, Conceptualization, Funding acquisition, Investigation, Validation, Writing – review and editing | Cécile Oury, Conceptualization, Data curation, Formal analysis, Funding acquisition, Investigation, Methodology, Project administration, Resources, Supervision, Validation, Writing – review and editing

DATA AVAILABILITY

Sequencing data of ticagrelor-resistant MRSA clones are available in BioProject under accession number [PRJNA1063881](#).

ADDITIONAL FILES

The following material is available [online](#).

Supplemental Material

Supplemental material (mBio01322-24-s0001.pdf). Supplemental materials and methods, Figures S1 to S7, Table S2, and movie legends.

Table S1 (mBio01322-24-s0002.xlsx). Lipidomics data.

Movie S1 (mBio01322-24-s0003.mp4). Untreated *B. subtilis*.

Movie S2 (mBio01322-24-s0004.mp4). *B. subtilis* with ticagrelor.

Movie S3 (mBio01322-24-s0005.mp4). *B. subtilis* with nisin.

REFERENCES

- Ventola CL. 2015. The antibiotic resistance crisis: part 1: causes and threats. *PT* 40:277–283.
- Antimicrobial Resistance Collaborators. 2022. Global burden of bacterial antimicrobial resistance in 2019: a systematic analysis. *Lancet* 399:629–655. [https://doi.org/10.1016/S0140-6736\(21\)02724-0](https://doi.org/10.1016/S0140-6736(21)02724-0)
- Fuller R, Chavez B. 2012. Ticagrelor (brilinta), an antiplatelet drug for acute coronary syndrome. *PT* 37:562–568.
- Springthorpe B, Bailey A, Barton P, Birkinshaw TN, Bonnert RV, Brown RC, Chapman D, Dixon J, Guile SD, Humphries RG, et al. 2007. From ATP to AZD6140: the discovery of an orally active reversible P2Y12 receptor antagonist for the prevention of thrombosis. *Bioorg Med Chem Lett* 17:6013–6018. <https://doi.org/10.1016/j.bmcl.2007.07.057>
- Wallentin L, Becker RC, Budaj A, Cannon CP, Emanuelsson H, Held C, Horrow J, Husted S, James S, Katus H, Mahaffey KW, Scirica BM, Skene A, Steg PG, Storey RF, Harrington RA, Freij A, Thorsén M, PLATO Investigators. 2009. Ticagrelor versus clopidogrel in patients with acute coronary syndromes. *N Engl J Med* 361:1045–1057. <https://doi.org/10.1056/NEJMoa0904327>
- Sexton TR, Zhang G, Macaulay TE, Callahan LA, Charnigo R, Vsevolozhskaya OA, Li Z, Smyth S. 2018. Ticagrelor reduces thromboinflammatory markers in patients with pneumonia. *JACC Basic Transl Sci* 3:435–449. <https://doi.org/10.1016/j.jacbts.2018.05.005>
- Phanchana M, Phetruen T, Harnvoravongchai P, Raksat P, Ounjai P, Chankhamhaengdech S, Janvilisri T. 2020. Repurposing a platelet aggregation inhibitor ticagrelor as an antimicrobial against *Clostridioides difficile*. *Sci Rep* 10:6497. <https://doi.org/10.1038/s41598-020-63199-x>
- Lancellotti P, Musumeci L, Jacques N, Servais L, Goffin E, Pirote B, Oury C. 2019. Antibacterial activity of ticagrelor in conventional antiplatelet dosages against antibiotic-resistant Gram-positive bacteria. *JAMA Cardiol* 4:596–599. <https://doi.org/10.1001/jamacardio.2019.1189>
- Oury C, Meyers S, Jacques N, Leeten K, Jiang Z, Musumeci L, Lox M, Debuissson M, Goffin E, Pirote B, Delvenne P, Nchimi A, Hubert C, Heptia M, Hubert P, Kuijpers MJE, Vanassche T, Martinod K, Verhamme P, Lancellotti P. 2023. Protective effect of ticagrelor against infective endocarditis induced by virulent *Staphylococcus aureus* in mice. *JACC Basic Transl Sci* 8:1439–1453. <https://doi.org/10.1016/j.jacbts.2023.02.003>
- Pant N, Miranda-Hernandez S, Rush C, Warner J, Eisen DP. 2022. Non-antimicrobial adjuvant therapy using ticagrelor reduced biofilm-related *Staphylococcus aureus* prosthetic joint infection. *Front Pharmacol* 13:927783. <https://doi.org/10.3389/fphar.2022.927783>
- Lupu L, Shepshelovich D, Banai S, Hershkovitz R, Isakov O. 2020. Effect of ticagrelor on reducing the risk of Gram-Positive infections in patients with acute coronary syndrome. *Am J Cardiol* 130:56–63. <https://doi.org/10.1016/j.amjcard.2020.06.016>
- Butt JH, Fosbøl EL, Gerds TA, Iversen K, Bundgaard H, Bruun NE, Larsen AR, Petersen A, Andersen PS, Skov RL, Østergaard L, Havers-Borgersen E, Gislason GH, Torp-Pedersen C, Køber L, Olesen JB. 2022. Ticagrelor and the risk of *Staphylococcus aureus* bacteraemia and other infections. *Eur Heart J Cardiovasc Pharmacother* 8:13–19. <https://doi.org/10.1093/ehjcvp/pvaa099>
- Urban A, Eckermann S, Fast B, Metzger S, Gehling M, Ziegelbauer K, Rübsamen-Waigmann H, Freiberg C. 2007. Novel whole-cell antibiotic biosensors for compound discovery. *Appl Environ Microbiol* 73:6436–6443. <https://doi.org/10.1128/AEM.00586-07>
- Wex KW, Saur JS, Handel F, Ortlieb N, Mokeev V, Kulik A, Niedermeyer THJ, Mast Y, Grond S, Berscheid A, Brötz-Oesterhelt H. 2021. Bioreporters for direct mode of action-informed screening of antibiotic producer strains. *Cell Chem Biol* 28:1242–1252. <https://doi.org/10.1016/j.chembiol.2021.02.022>
- Strahl H, Hamoen LW. 2010. Membrane potential is important for bacterial cell division. *Proc Natl Acad Sci U S A* 107:12281–12286. <https://doi.org/10.1073/pnas.1005485107>
- Sidders AE, Kedziora KM, Arts M, Daniel J-M, de Benedetti S, Beam JE, Bui DT, Parsons JB, Schneider T, Rowe SE, Conlon BP. 2023. Antibiotic-induced accumulation of lipid II synergizes with antimicrobial fatty acids to eradicate bacterial populations. *Elife* 12:e80246. <https://doi.org/10.7554/eLife.80246>
- Tiyanont K, Doan T, Lazarus MB, Fang X, Rudner DZ, Walker S. 2006. Imaging peptidoglycan biosynthesis in *Bacillus subtilis* with fluorescent antibiotics. *Proc Natl Acad Sci U S A* 103:11033–11038. <https://doi.org/10.1073/pnas.0600829103>
- McAuley S, Vadia S, Jani C, Huynh A, Yang Z, Levin PA, Nodwell JR. 2019. A chemical inhibitor of cell growth reduces cell size in *Bacillus subtilis*. *ACS Chem Biol* 14:688–695. <https://doi.org/10.1021/acscchembio.8b01066>
- Nonejuie P, Burkart M, Pogliano K, Pogliano J. 2013. Bacterial cytological profiling rapidly identifies the cellular pathways targeted by antibacterial molecules. *Proc Natl Acad Sci U S A* 110:16169–16174. <https://doi.org/10.1073/pnas.1311066110>
- Wong F, Stokes JM, Cervantes B, Penkov S, Friedrichs J, Renner LD, Collins JJ. 2021. Cytoplasmic condensation induced by membrane damage is associated with antibiotic lethality. *Nat Commun* 12:2321. <https://doi.org/10.1038/s41467-021-22485-6>
- Jensen C, Li H, Vestergaard M, Dalsgaard A, Frees D, Leisner JJ. 2020. Nisin damages the septal membrane and triggers DNA condensation in methicillin-resistant *Staphylococcus aureus*. *Front Microbiol* 11:1007. <https://doi.org/10.3389/fmicb.2020.01007>
- Lamsa A, Liu W-T, Dorrestein PC, Pogliano K. 2012. The *Bacillus subtilis* cannibalism toxin SDP collapses the proton motive force and induces autolysis. *Mol Microbiol* 84:486–500. <https://doi.org/10.1111/j.1365-2958.2012.08038.x>
- Engman J, Rogstam A, Frees D, Ingmer H, von Wachenfeldt C. 2012. The YjbH adaptor protein enhances proteolysis of the transcriptional regulator Spx in *Staphylococcus aureus*. *J Bacteriol* 194:1186–1194. <https://doi.org/10.1128/JB.06414-11>
- Stahlhut SG, Alqarzaee AA, Jensen C, Fisker NS, Pereira AR, Pinho MG, Thomas VC, Frees D. 2017. The ClpXP protease is dispensable for degradation of unfolded proteins in *Staphylococcus aureus*. *Sci Rep* 7:11739. <https://doi.org/10.1038/s41598-017-12122-y>
- Baker TA, Sauer RT. 2012. ClpXP, an ATP-powered unfolding and protein-degradation machine. *Biochim Biophys Acta* 1823:15–28. <https://doi.org/10.1016/j.bbamcr.2011.06.007>
- Short SA, White DC. 1971. Metabolism of phosphatidylglycerol, lysylphosphatidylglycerol, and cardiolipin of *Staphylococcus aureus*. *J Bacteriol* 108:219–226. <https://doi.org/10.1128/jb.108.1.219-226.1971>
- Koprivnjak T, Zhang D, Ernst CM, Peschel A, Nauseef WM, Weiss JP. 2011. Characterization of *Staphylococcus aureus* cardiolipin synthases 1 and 2 and their contribution to accumulation of cardiolipin in stationary phase and within phagocytes. *J Bacteriol* 193:4134–4142. <https://doi.org/10.1128/JB.00288-11>
- Ernst CM, Slavetinsky CJ, Kuhn S, Hauser JN, Nega M, Mishra NN, Gekeler C, Bayer AS, Peschel A. 2018. Gain-of-function mutations in the phospholipid flippase MprF confer specific daptomycin resistance. *MBio* 9:1–12. <https://doi.org/10.1128/mBio.01659-18>
- Jones T, Yeaman MR, Sakoulas G, Yang S-J, Proctor RA, Sahl H-G, Schrenzel J, Xiong YQ, Bayer AS. 2008. Failures in clinical treatment of *Staphylococcus aureus* infection with daptomycin are associated with alterations in surface charge, membrane phospholipid asymmetry, and drug binding. *Antimicrob Agents Chemother* 52:269–278. <https://doi.org/10.1128/AAC.00719-07>
- Xu L, Henriksen C, Mebus V, Guérillot R, Petersen A, Jacques N, Jiang J-H, Derks RJE, Sánchez-López E, Giera M, Leeten K, Stinear TP, Oury C, Howden BP, Peleg AY, Frees D. 2023. A clinically selected *Staphylococcus aureus* clpP mutant survives daptomycin treatment by reducing binding of the antibiotic and adapting a rod-shaped morphology. *Antimicrob Agents Chemother* 67:e0032823. <https://doi.org/10.1128/aac.00328-23>
- Tarai B, Das P, Kumar D. 2013. Recurrent challenges for clinicians: emergence of methicillin-resistant *Staphylococcus aureus*, vancomycin resistance, and current treatment options. *J Lab Physicians* 5:71–78. <https://doi.org/10.4103/0974-2727.119843>
- Jordan S, Junker A, Helmann JD, Mascher T. 2006. Regulation of LiaRS-dependent gene expression in *Bacillus subtilis*: identification of inhibitor proteins, regulator binding sites, and target genes of a conserved cell envelope stress-sensing two-component system. *J Bacteriol* 188:5153–5166. <https://doi.org/10.1128/JB.00310-06>

33. Pogliano J, Pogliano N, Silverman JA. 2012. Daptomycin-mediated reorganization of membrane architecture causes mislocalization of essential cell division proteins. *J Bacteriol* 194:4494–4504. <https://doi.org/10.1128/JB.00011-12>
34. Zhang L, Esquembre LA, Xia S-N, Oesterhelt F, Hughes CC, Brötz-Oesterhelt H, Teufel R. 2022. Antibacterial synnepyrroles from human-associated *Nocardiopsis* sp. show protonophore activity and disrupt the bacterial cytoplasmic membrane. *ACS Chem Biol* 17:2836–2848. <https://doi.org/10.1021/acscchembio.2c00460>
35. Cacace E, Kim V, Varik V, Knopp M, Tietgen M, Brauer-Nikonow A, Inecik K, Mateus A, Milanese A, Märli MT, Mitosch K, Selkrig J, Brochado AR, Kuipers OP, Kjos M, Zeller G, Savitski MM, Göttig S, Huber W, Typas A. 2023. Systematic analysis of drug combinations against Gram-positive bacteria. *Nat Microbiol* 8:2196–2212. <https://doi.org/10.1038/s41564-023-01486-9>
36. Engman J, von Wachenfeldt C. 2015. Regulated protein aggregation: a mechanism to control the activity of the ClpXP adaptor protein YjyB. *Mol Microbiol* 95:51–63. <https://doi.org/10.1111/mmi.12842>
37. Frees D, Qazi SNA, Hill PJ, Ingmer H. 2003. Alternative roles of ClpX and ClpP in *Staphylococcus aureus* stress tolerance and virulence. *Mol Microbiol* 48:1565–1578. <https://doi.org/10.1046/j.1365-2958.2003.03524.x>
38. Moreno-Cinos C, Goossens K, Salado IG, Van Der Veken P, De Winter H, Augustyns K. 2019. ClpP protease, a promising antimicrobial target. *Int J Mol Sci* 20:2232. <https://doi.org/10.3390/ijms20092232>
39. Bæk KT, Gründling A, Mogensen RG, Thøgersen L, Petersen A, Paulander W, Frees D. 2014. β -lactam resistance in methicillin-resistant *Staphylococcus aureus* USA300 is increased by inactivation of the ClpXP protease. *Antimicrob Agents Chemother* 58:4593–4603. <https://doi.org/10.1128/AAC.02802-14>
40. Pamp SJ, Frees D, Engelmann S, Hecker M, Ingmer H. 2006. Spx is a global effector impacting stress tolerance and biofilm formation in *Staphylococcus aureus*. *J Bacteriol* 188:4861–4870. <https://doi.org/10.1128/JB.00194-06>
41. Nielsen TK, Petersen IB, Xu L, Barbuti MD, Mebus V, Justh A, Alqarzaee AA, Jacques N, Oury C, Thomas V, Kjos M, Henriksen C, Frees D. 2024. The Spx stress regulator confers high-level β -lactam resistance and decreases susceptibility to last-line antibiotics in methicillin-resistant *Staphylococcus aureus*. *bioRxiv:2024.03.01.582999*. <https://doi.org/10.1101/2024.03.01.582999>
42. Grein F, Müller A, Scherer KM, Liu X, Ludwig KC, Klöckner A, Strach M, Sahl H-G, Kubitscheck U, Schneider T. 2020. Ca^{2+} -daptomycin targets cell wall biosynthesis by forming a tripartite complex with undecaprenyl-coupled intermediates and membrane lipids. *Nat Commun* 11:1455. <https://doi.org/10.1038/s41467-020-15257-1>
43. Hachmann A-B, Sevim E, Gaballa A, Popham DL, Antelmann H, Helmann JD. 2011. Reduction in membrane phosphatidylglycerol content leads to daptomycin resistance in *Bacillus subtilis*. *Antimicrob Agents Chemother* 55:4326–4337. <https://doi.org/10.1128/AAC.01819-10>
44. Ernst CM, Peschel A. 2011. Broad-spectrum antimicrobial peptide resistance by MprF-mediated aminoacylation and flipping of phospholipids. *Mol Microbiol* 80:290–299. <https://doi.org/10.1111/j.1365-2958.2011.07576.x>
45. Jung D, Rozek A, Okon M, Hancock REW. 2004. Structural transitions as determinants of the action of the calcium-dependent antibiotic daptomycin. *Chem Biol* 11:949–957. <https://doi.org/10.1016/j.chembiol.2004.04.020>
46. Müller A, Wenzel M, Strahl H, Grein F, Saaki TNV, Kohl B, Siersma T, Bandow JE, Sahl HG, Schneider T, Hamoen LW. 2016. Daptomycin inhibits cell envelope synthesis by interfering with fluid membrane microdomains. *Proc Natl Acad Sci U S A* 113:E7077–E7086. <https://doi.org/10.1073/pnas.1611173113>
47. Ernst CM, Peschel A. 2019. MprF-mediated daptomycin resistance. *Int J Med Microbiol* 309:359–363. <https://doi.org/10.1016/j.ijmm.2019.05.010>
48. Maron B, Rolff J, Friedman J, Hayouka Z. 2022. Antimicrobial peptide combination can hinder resistance evolution. *Microbiol Spectr* 10:e0097322. <https://doi.org/10.1128/spectrum.00973-22>
49. Song D, Jiao H, Liu Z. 2021. Phospholipid translocation captured in a bifunctional membrane protein MprF. *Nat Commun* 12:2927. <https://doi.org/10.1038/s41467-021-23248-z>
50. Choo EJ, Chambers HF. 2016. Treatment of methicillin-resistant *Staphylococcus aureus* bacteremia. *Infect Chemother* 48:267–273. <https://doi.org/10.3947/ic.2016.48.4.267>
51. Stülke J, Hanschke R, Hecker M. 1993. Temporal activation of β -glucanase synthesis in *Bacillus subtilis* is mediated by the GTP pool. *J Gen Microbiol* 139:2041–2045. <https://doi.org/10.1099/00221287-139-9-2041>
52. Otani H, Mouncey NJ. 2022. RIVIT-seq enables systematic identification of regulons of transcriptional machineries. *Nat Commun* 13:3502. <https://doi.org/10.1038/s41467-022-31191-w>
53. Matyash V, Liebisch G, Kurzchalia TV, Shevchenko A, Schwudke D. 2008. Lipid extraction by methyl-tert-butyl ether for high-throughput lipidomics. *J Lipid Res* 49:1137–1146. <https://doi.org/10.1194/jlr.D700041-JLR200>
54. Kong L, Dawkins E, Campbell F, Winkler E, Derks RJE, Giera M, Kamp F, Steiner H, Kros A. 2020. Photo-controlled delivery of very long chain fatty acids to cell membranes and modulation of membrane protein function. *Biochim Biophys Acta Biomembr* 1862:183200. <https://doi.org/10.1016/j.bbamem.2020.183200>